10th IMEKO TC10 Conference on
Technical Diagnostics
Budapest, HUNGARY, 2005, June 09-10

BEARING FAULT DETECTION FOR ON-LINE QUALITY CONTROL OF ELECTRIC MOTORS

Jiří Vass[*], *Cristina Cristalli*[**]

[*] Czech Technical University, FEE, Dept. of Circuit Theory, Prague, Czech Republic
[**] The Loccioni Group, AEA s.r.l., Angeli di Rosora (Ancona), Italy

Abstract – This paper is concerned with analysis and classification of vibration signals from universal electric motors. The goal is to reveal manufacturing defects caused by assembly machines composing the motors on a production line. Such machines may under certain conditions use inappropriate force, and hence cause a mechanical shock, resulting in a damage of the motor bearings. The proposed system comprises a preprocessor based on continuous wavelet transform in order to reduce the noise masking the characteristic frequencies of bearing faults. The noise reduction is based on the adaptive Morlet wavelet and soft-thresholding of wavelet coefficients. Individual blocks of the preprocessor are presented and important practical issues are considered, such as segmentation and proper selection of wavelet scales. Identification of defective motors is performed by a simple and effective technique based on autocorrelation function, utilizing prior information on vibration frequency features. Finally, two error measures are designed in order to evaluate influence of a simulated noise level on efficiency of the fault diagnosis system. Achieved results appear to be promising and applicable in automatic quality control.

Keywords: rolling bearing, vibration analysis, continuous wavelet transform

1. INTRODUCTION

In many domestic and industrial applications, rolling element bearings are regarded as critical mechanical components with strong influence on functionality of rotating machinery. For this reason, various measurement methods have been developed [1] with the aim of detection and identification of faults in bearings. Among these methods, vibration analysis has been established as the most common and reliable technique, though vibration signals are often distorted due to noisy environmental conditions, such as on production lines. Therefore, noise removal from measured signals is an essential step in robust detection of mechanical defects.

For the last 10 years, wavelet transform has successfully been applied in vibration signal analysis and fault detection. Indeed, recently published diagnosis systems often consist of a signal preprocessor based on wavelets [2-4]. In addition, a new denoising algorithm based on the adaptive Morlet wavelet has recently been proposed [5], and further extended in our previous work [6]. This paper presents a complete vibrodiagnostic system, consisting of the improved wavelet preprocessor, as well as a novel classifier based on periodicity recognition.

The proposed system is described in Sections 2-5. In Section 2, acquisition of vibration signals is discussed. In Section 3, individual blocks of the wavelet-based preprocessor are examined. Sections 4 and 5 are concerned with the feature extractor and the classifier, respectively. In Section 6, error measures are designed and simulation results are presented. The conclusion is given in Section 7.

2. DATA ACQUISITION

Vibrations of examined motors were measured by a contactless optical method (Fig. 1). In particular, velocity of surface vibrations was measured by a digital vibrometer based on the Laser Doppler Velocimetry (LDV) technology, providing several advantages over standard accelerometer measurements [7]. Vibration signals were acquired during the stationary (steady) state with a rotational speed of 1000 rpm (16,6 Hz), during which the laser beam was aimed on the upper or the lower bearing of the motor.

All tested motors were universal AC motors employed in commercial washing machines. As can be observed, the shaft of the analyzed motor is vertically oriented in order to achieve constant load on each rolling element. Data was measured for 2 seconds with a sampling frequency of 50 kHz.

Fig. 1. Measurement of bearing vibrations using a laser vibrometer

It is well known that vibration signals of faulty bearings comprise a periodic impulse train with a period corresponding to a specific bearing fault. A typical fault is a small pit on the surface of the outer bearing raceway, causing generation of impulses as rolling elements (balls) pass over the pit. Fault characteristic frequencies can theoretically be calculated from specifications of the particular bearing type using the following equations [1, 8]:

$$f_{bpo} = \frac{N_b}{2} f_r \left(1 - \frac{D_b \cos\theta}{D_c} \right) \approx 0,4 \cdot f_r \cdot N_b , \qquad (1)$$

$$f_{bpi} = \frac{N_b}{2} f_r \left(1 + \frac{D_b \cos\theta}{D_c} \right) \approx 0,6 \cdot f_r \cdot N_b , \qquad (2)$$

$$f_c = \frac{1}{2} f_r \left(1 - \frac{D_b \cos\theta}{D_c} \right) \approx 0,4 \cdot f_r , \qquad (3)$$

$$f_b = \frac{D_c}{2D_b} f_r \left(1 - \frac{D_b^2 \cos^2\theta}{D_c^2} \right), \qquad (4)$$

where f_{bpo} is the ball pass outer raceway frequency, f_{bpi} is the ball pass inner raceway frequency, f_c is the fundamental cage frequency, f_b is the ball rotational frequency, f_r is the shaft rotational frequency, N_b is the number of bearing balls, D_b is the ball diameter, D_c is the cage diameter, and θ is the contact angle. The approximate formulas [8] are useful for applications with unknown contact angle.

3. WAVELET DENOISING

Due to an extensive noise in industrial applications, denoising of the measured vibration signals is a fundamental step to be performed prior to an automatic identification of bearing faults. Therefore, we have employed the wavelet-based approach by Lin and Qu [5], and derived an important modification to guarantee stability of the algorithm [6]. This improvement is embedded in the signal preprocessor described in this section. Furthermore, individual blocks of the system are considered in detail and some important practical issues are discussed. Detailed scheme of the preprocessor is depicted in Fig. 2, whereas Table I provides an explanation of the variables in the diagram.

3.1. Principle of the method

Filtering of noisy vibration signals is based on continuous wavelet transform (CWT) and noise reduction by thresholding of wavelet coefficients. Therefore, the most important parts of the preprocessor are the CWT block, the Thresholding block, and the ICWT (Inverse CWT) block.

The denoising procedure can conveniently be described by four basic steps illustrated in Fig. 3. Fig. 3(a) shows a simulated vibration signal corrupted by a significant level of additive white Gaussian noise. The characteristic impulse train cannot be observed since it is buried in the noise. On the other hand, Fig. 3(b) presents a scalogram of the noisy vibration signal, in which the periodic impulses are distinguishable from the noise. Note that the vertical axis is labelled with frequency in Hz (instead of wavelet scales) in order to simplify interpretation of the CWT. Fig. 3(d) displays the scalogram after application of thresholding in the wavelet domain. As a result, large wavelet coefficients corresponding to impulses are preserved, while small coefficients representing the noise have significantly been decreased. Finally, the denoised impulse signal in Fig. 3(c) is reconstructed by the inverse CWT.

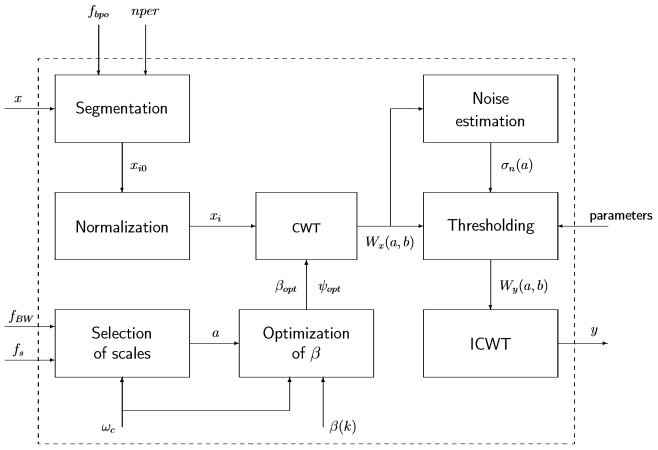

Fig. 2. Block diagram of the wavelet preprocessor

TABLE I. Description of variables in the denoising algorithm

Symbol	Description
x	noisy vibration signal
f_s	signal sampling frequency [Hz]
f_{BW}	frequency range of interest [Hz]
f_{bpo}	fault characteristic frequency [Hz]
n_{per}	number of impulses in a segment
x_{i0}	segment of x
x_i	normalized segment of x
ω_c	center frequency of $\psi(t)$ [rad/s]
a	vector of wavelet scales
$\beta(k)$	admissible values of β
β_{opt}	optimal value of parameter β
ψ_{opt}	optimally adapted Morlet wavelet
$W_x(a,b)$	noisy scalogram
$W_y(a,b)$	thresholded scalogram
$\sigma_n(a)$	estimates of noise std
y	denoised vibration signal

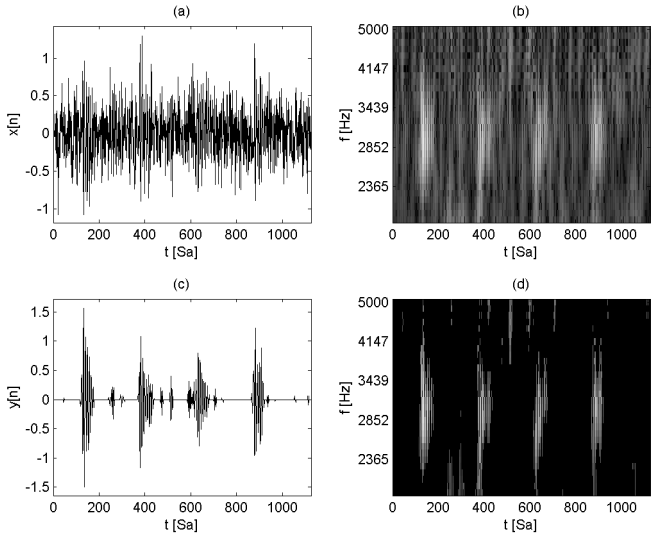

Fig. 3. Denoising in the wavelet domain: (a) noisy vibration signal. (b) scalogram of the noisy signal. (c) reconstructed signal. (d) thresholded scalogram.

Essential task in application of wavelets is an appropriate selection of the mother wavelet $\psi(t)$. Lin and Qu [5] proposed to employ the Morlet wavelet [9], since its shape is similar to an impulse, a common symptom of faults in various mechanical systems. This important similarity yields high correlation between the mother wavelet and the impulse signal to be extracted, resulting in visual magnification of impulses in the CWT scalogram (Fig. 3(b)) and representation by a small number of large wavelet coefficients. On the contrary, noise is uncorrelated with the Morlet wavelet, which leads to a representation by a large number of small CWT coefficients. As a consequence, noise can efficiently be suppressed in the Thresholding block by means of the soft-thresholding rule [10].

3.2 Segmentation and normalization

The Segmentation block divides the entire measured signal into shorter portions to be denoised and then analyzed in the classifier. Each signal portion is further segmented (windowed) in the CWT block, since the segmentation block only computes the necessary portion length (in samples) according to (5). This length guarantees that each portion of a vibration signal contains the desired number of impulses n_{per}, repeated with a theoretical characteristic period of N_{bpo} samples.

$$N_{xi} = n_{per} \cdot N_{bpo} = n_{per} \cdot \frac{f_s}{f_{bpo}}. \qquad (5)$$

The Normalization block removes the DC offset, and normalizes each segment to the unit power.

3.3 Selection of wavelet scales

This issue appears to be somewhat neglected in literature, although proper selection of wavelet scales plays an important role in the denoising process. Indeed, selected scales should correspond to a frequency band containing the bearing resonance frequency f_{res}. Therefore, the denoising system requires an additional input of a frequency band of interest:

$$f_{BW} = \left[f_{min}, f_{max} \right] \qquad f_{res} \in f_{BW}. \qquad (6)$$

For example, the frequency band from 2 kHz to 5 kHz should adequately cover a typical resonance frequency of 3 kHz. Moreover, proper scales should constitute a sufficiently fine grid of frequencies around f_{res}, and it is thus desirable to use a power of 2 series of scales, instead of a linear grid. This idea [11, 3] has been extended in our system to compute the vector of dilations $\underline{a}$ as follows:

$$a_{min} = \frac{f_c \cdot f_s}{f_{max}} \qquad a_{max} = \frac{f_c \cdot f_s}{f_{min}}, \qquad (7)$$

$$\Delta a = \log_2(a_{max}) - \log_2(a_{min}), \qquad (8)$$

$$J = \frac{1}{dj} \cdot \Delta a, \qquad (9)$$

$$\underline{a} = a_{min} \cdot 2^{j \cdot dj}, \quad j = 0, 1, \ldots J. \qquad (10)$$

J is the total number of scales, whereas dj determines a "scale step", and can be chosen as a reciprocal value of the DFT frequency bin, i.e. $dj = (f_s/N)^{-1}$. Provided that reasonable frequency band f_{BW} is given, this selection of scales should guarantee that the resulting scalogram sufficiently highlights the impulsive components in the vibration signal.

3.4 Optimization of the parameter β

This block is concerned with optimization of the bandwidth parameter β controlling the time-frequency resolution of the Morlet wavelet. This task is a key point in the preprocessing, as it significantly influences the success of the denoising algorithm. For this reason, Lin and Qu [5] proposed a technique for finding the optimal value of β, referred to as the wavelet entropy criterion. However, our research [6] revealed a substantial drawback of this approach, demanding a redefinition of the Morlet wavelet:

$$\psi(t) = \left(\frac{\beta}{2\pi} \cdot e^{-\beta^2 t^2/2} \right) \cdot \cos(\omega_c t), \qquad (11)$$

where $\omega_c = 7\pi/4$ rad/s and the adaptive parameter β must be optimized only within a limited interval < 0,52 ; 1,83 >.

3.5 Noise Estimation

The Noise Estimation block is based on MAD (Median Absolute Deviation) of the wavelet coefficients [9]. In particular, MAD/0,6745 is an estimate of the noise standard deviation (std) $\sigma_n(a)$, calculated for each wavelet scale a. Subsequently, the estimated noise level $\sigma_n(a)$ determines the threshold value utilized in the Thresholding block.

4. FEATURE EXTRACTION

Feature extractor in Fig. 4 analyzes the denoised vibration signal obtained from the wavelet preprocessor. Since vibrations of faulty motors contain periodically repeated impulses, the distinction between good and faulty bearings is based on periodicity detection using the autocorrelation function (ACF) of the vibration signal.

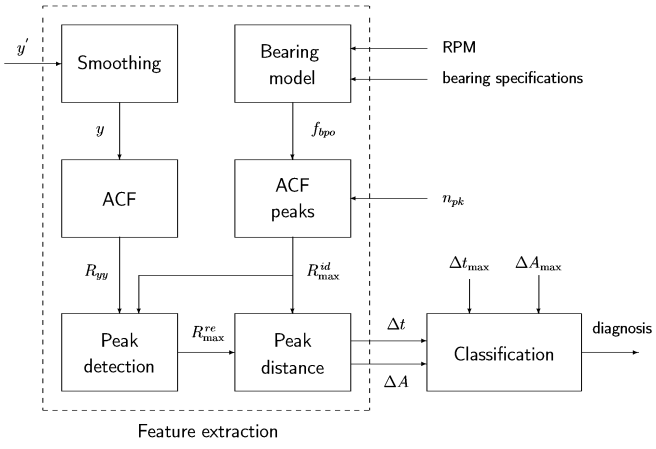

Fig. 4. Block diagram of the feature extractor and classifier

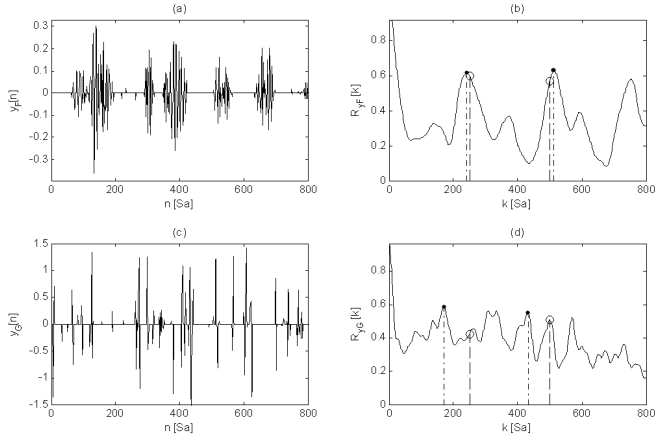

Fig. 5: Denoised vibration signals and the corresponding auto-correlation functions: (a) signal y_F from a faulty motor. (b) ACF of y_F. (c) signal y_G from a good motor. (d) ACF of y_G. Real and theoretical autocorrelation maxima are depicted as dots and circles, respectively. Number of compared ACF peaks $n_{pk} = 2$.

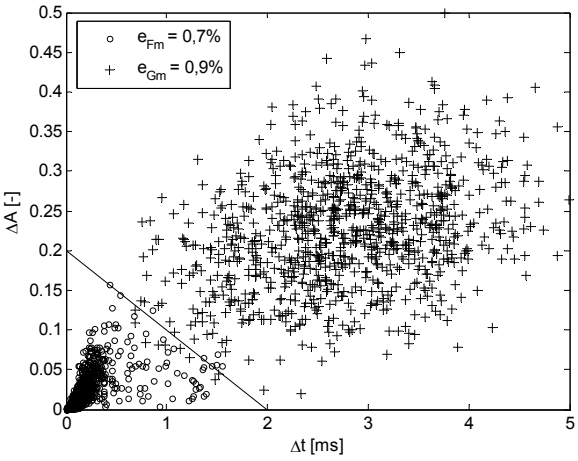

Fig. 6: Classification of motors in the feature space. Good and faulty motors are depicted as crosses and circles, respectively.

Fig. 5 displays a typical denoised signal from a good and faulty motor, as well as the corresponding autocorrelation functions. As shown in Fig. 5(b), $R_{yF}[k]$ comprises large maxima corresponding to a fault characteristic frequency, such as f_{bpo}. Since this frequency can be computed using (1), we can measure the distance between the theoretical and the real autocorrelation maxima. The theoretical (ideal) maxima are provided by the ACF peaks block, which computes the desired number of peaks n_{pk} using the characteristic period N_{bpo} in samples:

$$R_{max}^{id}[p] = p \cdot N_{bpo} = p \cdot \frac{f_s}{f_{bpo}} \qquad p = 1, 2, ..., n_{pk} . \quad (12)$$

The input signal is low-pass filtered in the Smoothing block, in order to remove fluctuations of the autocorrelation function for easier detection of the real ACF maxima. Afterwards, both ideal and real maxima are processed in the Peak distance block computing their average difference in time and amplitude:

$$\left[\Delta t_p, \Delta A_p\right] = \left| R_{max}^{id}[p] - R_{max}^{re}[p] \right| \qquad p = 1, 2, ..., n_{pk} , \quad (13)$$

$$\Delta t = \frac{1}{n_{pk}} \sum_{p=1}^{n_{pk}} \Delta t_p \qquad \Delta A = \frac{1}{n_{pk}} \sum_{p=1}^{n_{pk}} \Delta A_p . \quad (14)$$

Finally, these two distance measures form the feature vector $F = (F_1, F_2) = (\Delta t, \Delta A)$ utilized in the classifier.

5. CLASSIFICATION

Classification of motors operates in a two-dimensional feature space (Fig. 6), which consists of points obtained by mapping the extracted features $(\Delta t, \Delta A)$. Therefore, the horizontal coordinate is the time difference Δt in the position of autocorrelation maxima, whereas the vertical coordinate is formed by the difference ΔA in the amplitude.

As illustrated in Fig. 5(b), faulty motors are characterized by a small difference in autocorrelation peaks, and are thus mapped close to the origin $(\Delta t, \Delta A) \rightarrow [0,0]$. On the other hand, denoised vibration signals from good motors are formed only by random impulses of the remaining motor noise (Fig. 5(c)). Hence, the period of impulses is also random, resulting in a large distance of the real autocorrelation peaks from their theoretical counterparts. As a result, good motors tend to be mapped far from the origin of the feature space, as shown in Fig. 6. Based on this concept, good and faulty motors can linearly be separated using a discrimination line, controlled by a selection of maximum allowable differences Δt_{max} and ΔA_{max} (Fig. 4). As the position of this line represents sensitivity of the classifier, it can specifically be adjusted by a manufacturer according to the desired standard of production quality.

6. SIMULATION RESULTS

Vibration signals from faulty motors were generated as a periodic train of exponentially decaying impulses [12] with a typical fault frequency f_{bpo}. Then, the impulse signal was distorted by 1000 realizations of white Gaussian noise for a signal-to-noise ratio (SNR) ranging from 0 to -10 dB. On the contrary, signals from good motors were simulated as a pure noise, thus obtaining the total number of 2000 test signals.

Two simple error measures are defined for evaluation of the diagnosis system. First, error in faulty motors e_{Fm} indicating in percentage how many faulty motors are incorrectly classified as good motors. Second, error in good motors e_{Gm} analogically expressing the portion of good motors considered as faulty due to an error of the diagnosis system.

Our experiments suggest that this method can reliably be applied for a maximum theoretical value of SNR = -5 dB, with e_{Fm} = 0,72 % and e_{Gm} = 0,91 % (Fig. 6). When this SNR is exceeded, faulty motors are mapped across the discrimination line into the region of good motors, resulting in a rapid increase of e_{Fm}, although e_{Gm} remains relatively low, as given in Table II. This indicates a failure of the wavelet preprocessor to suppress the noise of excessively high level, and impossibility to extract the impulse signal. For this reason, it is important to minimize the noise induced by the measurement method, in order to allow extraction of weak impulses typical for an early stage of a bearing fault.

TABLE II. Influence of noise level on classification errors

SNR [dB]	e_{Fm} [%]	e_{Gm} [%]
0	0,0	0,0
-1	0,1	0,2
-2	0,3	0,5
-3	0,4	0,6
-4	0,6	0,8
-5	0,7	0,9
-6	3,7	1,7
-7	9,9	2,6
-8	16,5	2,9
-9	28,9	3,8
-10	51,4	4,7

7. CONCLUSIONS

This paper presents an automatic system for fault diagnosis of mechanical defects in rolling element bearings. The diagnosis system consists of two principal parts: a wavelet-based preprocessor for denoising of vibration signals, and a classifier based on the autocorrelation function.

The preprocessing technique employs the optimized Morlet wavelet with adaptive time-frequency resolution, and suppresses the undesired noise by means of soft-thresholding in the wavelet domain. Several practical issues are considered, particularly the selection of wavelet scales is discussed in detail.

The proposed classifier utilizes extracted features obtained as distances between real and theoretical maxima of the autocorrelation function. The real autocorrelation maxima are detected in the denoised vibration signal by means of a smoothing filter and a simple peak detection technique. The theoretical autocorrelation maxima are obtained using the well-known fault characteristic frequencies, calculated from a bearing specification and a rotational speed of a motor.

Simulation study has been designed in order to estimate the maximum level of environmental noise that can be suppressed by the preprocessor to provide reliable features to the classifier. The achieved maximum value of SNR seems satisfactory for future application in an on-line quality control. Although the examined vibration signals are from universal motors in washing machines, the proposed method can be applied in diagnostics of other mechanical systems, such as gearboxes.

ACKNOWLEDGEMENTS

This work has been supported by the GA ČR grant No. 102/03/H085 ”Biological and Speech Signal Modelling” and the research program MSM6840770014 ”Research in the Area of the Prospective Information and Navigation Technologies”. This research is supervised by Prof. Ing. Pavel Sovka, CSc., Department of Circuit Theory, FEE CTU and Ing. Radislav Šmíd, Ph.D., Department of Measurement, FEE CTU. A special thanks goes to Barbara Torcianti for valuable discussions, as well as measurement of the vibration data.

REFERENCES

[1] N. Tandon, A. Choudhury, "A review of vibration and acoustic measurement methods for the detection of defects in rolling element bearings", *Tribology International*, vol. 32, pp. 469-480, 1999.

[2] B.A. Paya, I.I. Esat, M.N.M. Badi, "Artificial neural network based fault diagnostics of rotating machinery using wavelet transforms as a preprocessor", *Mechanical Systems and Signal Processing*, vol. 11, no. 5, pp. 751-765, 1997.

[3] H. Zheng, Z. Li, X. Chen, "Gear fault diagnosis based on continuous wavelet transform", *Mechanical Systems and Signal Processing*, , vol. 16, no. 2-3, pp. 47-457, 2002.

[4] X. Lou, K.A. Loparo, "Bearing fault diagnosis based on wavelet transform and fuzzy inference", *Mechanical Systems and Signal Processing*, vol. 18, no. 5, pp. 1077-1095, 2004.

[5] J. Lin, L. Qu, "Feature extraction based on Morlet wavelet and its application for mechanical fault diagnosis", *Journal of Sound and Vibration*, vol. 234 (1), pp. 135-148, 2000.

[6] J. Vass, C. Cristalli, "Optimization of Morlet wavelet for mechanical fault diagnosis", *Proceedings of the Twelfth International Congress on Sound and Vibration (ICSV12)*, Lisbon, Portugal, 8 pages (in press), July 2005. `http://amber.feld.cvut.cz/users/vass/ICSV12.pdf`

[7] R.M. Rodriguez, C. Cristalli, N. Paone, "Comparative study between laser vibrometer and accelerometer measurements for mechanical fault detection of electric motors", *SPIE Proceedings*., vol. 4827, pp. 521-529, 2002.

[8] A.V. Barkov, N.A. Barkova, "The artificial intelligence systems for machine condition monitoring and diagnostics by vibration", *Proceedings of Russian Federation Power Industry and Vibration Institute, USA*, vol. 9, Saint Petersburg, 1999.

[9] J. Morlet, G. Arens, E. Fourgeau, D. Giard, "Wave propagation and sampling theory - Part II: Sampling theory and complex waves", *Geophysics*, vol. 47, pp. 203-236, 1982.

[10] D.L. Donoho, "Wavelet shrinkage and W.V.D. -- A ten-minute tour", *Proceedings of the International Conference on Wavelets and Applications*, Toulouse, France, June 1992.

[11] C. Torrence, G.P. Compo, "A practical guide to wavelet analysis", *Bulletin of the American Meteorological Society*, vol. 79, no. 1, pp. 61–78, 1998.

[12] Y.-T. Sheen, "A complex filter for vibration signal demodulation in bearing defect diagnosis", *Journal of Sound and Vibration*, vol. 276, no. 1-2, pp. 105-119, 2004.

AUTHORS: Ing. Jiří Vass
CTU, FEE, Department of Circuit Theory
Technická 2, 166 27 Prague, Czech Republic
E-mail: vassj@fel.cvut.cz
Phone: +420-2-2435-2286

Dr. Cristina Cristalli
The Loccioni Group, AEA s.r.l.
Via Fiume 16, 60030 Angeli di Rosora (AN), Italy
E-mail: c.cristalli@loccioni.com
Phone: +39-0731-8161